Journal of Power Sources 198 (2012) 36–41

Contents lists available at SciVerse ScienceDirect

Journal of Power Sources

journal homepage: www.elsevier.com/locate/jpowsour

Enhanced anode interface for electrochemical oxidation of solid fuel in direct carbon fuel cells: The role of liquid Sn in mixed state

HyungKuk Ju[a], Sunghyun Uhm[b], Jin Won Kim[a], Rak-Hyun Song[c], Hokyung Choi[d], Si-Hyun Lee[d], Jaeyoung Lee[a,b,*]

[a] Electrochemical Reaction and Technology Laboratory, School of Environmental Science and Engineering, GIST, Gwangju 500-712, South Korea
[b] Ertl Center for Electrochemistry and Catalysis, Research Institute for Solar and Sustainable Energies (RISE), GIST, Gwangju 500-712, South Korea
[c] Fuel Cell Center, Korea Institute of Energy Research (KIER), Daejeon 305-343, South Korea
[d] Clean Fossil Energy Research Center, Korea Institute of Energy Research (KIER), Daejeon 305-343, South Korea

ARTICLE INFO

Article history:
Received 20 July 2011
Received in revised form
22 September 2011
Accepted 23 September 2011
Available online 1 October 2011

Keywords:
Direct carbon fuel cell
Liquid Sn anode
Electrochemical oxidation
Solid fuel
Enhanced anode interface

ABSTRACT

The role of liquid Sn in a direct carbon fuel cell with a Ni–yttria-stabilized zirconia (YSZ) cermet anode is investigated in terms of enhancing the solid fuel-to-solid anode interface and intrinsic electrocatalytic activity. Sn-mixed carbon black particles undergo a transformation from solid to liquid phase as the cell temperature rises, thereby leading to the formation of more favorable interface between carbon fuels, liquid Sn, and Ni–YSZ anodes. Moreover, additional Ni-impregnated Sn–carbon fuels show that further improvements in cell performance can be achieved by increasing the oxidation of carbon to CO. As a result, we observe a maximum power density of 60.5 and 105 mW cm^{-2} at 900 °C by using Sn–carbon and Ni–Sn–carbon fuels, respectively.

1. Introduction

Coal is the most abundant and widely distributed fossil fuel, is second in terms of being a primary energy source (with 27% of world demand), and is a major source of electricity generation by thermal power plants (41%, globally) [1,2]. Therefore, significant improvements in the coal fuel conversion and utilization efficiencies of power generation systems are needed in order to reduce the possible problem of global warming. In an attempt to resolve this matter, direct carbon fuel cells (DCFCs) are a promising novel electrochemical power source for central plants and even portable applications [3–5]. DCFCs can convert chemical energy directly into electric energy and thereby utilize various types of carbon sources; these sources can be derived from coal, coke, natural gas, petroleum, refining by-products, and even biomass. The overall cell reaction in DCFCs is the electrochemical oxidation of carbon to carbon dioxide (CO_2):

$$C + O_2 \rightarrow CO_2 \quad E^\circ = 1.02\,V \tag{1}$$

In the 19th century, the development of an electrochemical system and a demonstration of generating electricity via DCFCs were first attempted [6,7]. At present, DCFCs can be divided into three types: molten hydroxides [8,9], molten carbonates [10–12], and solid oxides [4,13–23] according to the electrolytes used. Most of these approaches have focused on the direct electrochemical oxidation of solid carbon fuel with no additional reforming process. However, the electrochemical reaction of solid carbon or coal has intrinsic properties of a large activation energy (26 kcal mol^{-1}) and slow kinetics at the anode [11,24,25]. To overcome these anode polarizations, the use of a solid oxide electrolyte such as yttria-stabilized zirconia (YSZ) has recently been proposed in DCFCs; advantages of YSZ include a relatively higher reaction activity and increased fuel flexibility due to its higher operation temperatures in the range of 600–1000 °C. In the case of simple arrangements, Nakagawa et al. [13] and Gür et al. [18] reported that solid carbon fuels should be placed onto the solid YSZ electrolyte in DCFCs, even though the main reaction leads to formation of CO by the reverse Boudouard reaction ($C + CO_2 \rightarrow CO$). Similarly, for direct physical contact between a solid fuel and anode, previous studies have reported that a very low power density (<20 mW cm^{-2}) was observed since the oxidation of carbon at the three-phase boundary (TPB) is limited due to its poor contact [21–23]. The electrochemical oxidation of fuels can only occur at the TPB, i.e., the interface

* Corresponding author at: Electrochemical Reaction and Technology Laboratory, School of Environmental Science and Engineering, GIST, Gwangju 500-712, South Korea. Tel.: +82 62 715 2440/2579; fax: +82 62 715 2434.
E-mail address: jaeyoung@gist.ac.kr (J. Lee).

0378-7753/$ – see front matter © 2011 Elsevier B.V. All rights reserved.
doi:10.1016/j.jpowsour.2011.09.082

between reactant (fuel), electrode (electronic conductor and catalyst), and electrolyte (ionic conductor) materials. In addition, due to the nature of carbon, the reactivity and fluidity of solid carbon fuels are much lower than those of gaseous fuels, which have a dimensional mismatch and size incompatibility between carbon particles and anode pores at the TPB [4,19,26].

Currently, Ihara et al. [4,14–16] and Li et al. [23] proposed a rechargeable direct carbon fuel cell (RDCFC) in which the carbon source is deposited via the thermal decomposition of gaseous hydrocarbon fuels such as propane and methane. The solid fuel could be well supplied at the TPB with a maximum power density of 55 mW cm^{-2} at 900 °C [15]. Gür et al. [19–21] integrated a fluidized-bed DCFC with a Boudouard-type dry gasifier and demonstrated a maximum power density of 170 mW cm^{-2} at 850 °C.

An alternative strategy for overcoming the intrinsic difficulties in applying an electrochemical reaction directly between solid carbons and a solid anode was developed by using liquid (molten) metals such as Fe [27], Ag [28], and Sn [29–33] as an anode in conjunction with a solid electrolyte. CellTech Power's liquid tin anode solid oxide fuel cell (LTA-SOFC) was shown to operate on various carbonaceous fuels without requiring further fuel reforming or processing. Of late, the cell achieved a maximum power density of 170 mW cm^{-2} on hydrogen and JP-8 (jet fuel) [33].

The concept of a liquid anode seems to have considerable merit. However, information pertaining to the effects of liquid Sn in DCFCs on carbon oxidation and Sn/SnO_2 redox mechanisms remains quite limited. In this study, we first investigate the role of liquid Sn mixed in solid carbon fuels at the Ni–YSZ cermet anode and the electrochemical oxidation mechanism for solid carbon fuels in DCFCs is also discussed. To expand this investation, additional Ni metal is impregnated into Sn–carbon fuels and further improvemets in cell performance are then investigated.

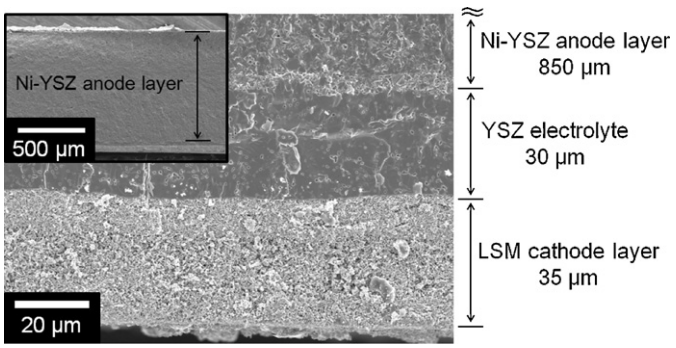

Fig. 1. Cross-sectional SEM image of an anode-supported button cell.

2. Experimental

In the DCFC system, anode-supported SOFC button cells (Ceramic Fuel Cell Power, Korea) were used, as shown in Fig. 1. The cell consisted of a porous Ni–YSZ anode (850 μm), a dense 8 mol % YSZ electrolyte (30 μm), and a porous lanthanum strontium manganate (LSM) cathode layer (35 μm). The diameter of the whole cell was 3 cm and the active area corresponding to the cathode layer was 0.75 cm^2.

In order to compare the differences in DCFC performance, three fuel samples were investigated. A commercial carbon black (ENSACO 350G, Timcal, Switzerland) with an average particle size of 50 nm and a specific surface area (BET) of 770 $m^2\,g^{-1}$ was selected as the primary fuel. As a secondary fuel, Sn powder (99%, Aldrich) was mixed with carbon black (Sn:C = 1:3 by weight ratio) to enhance the electrochemical reaction at the anode interface. An additional 6 wt.% of Ni was impregnated into the as-prepared

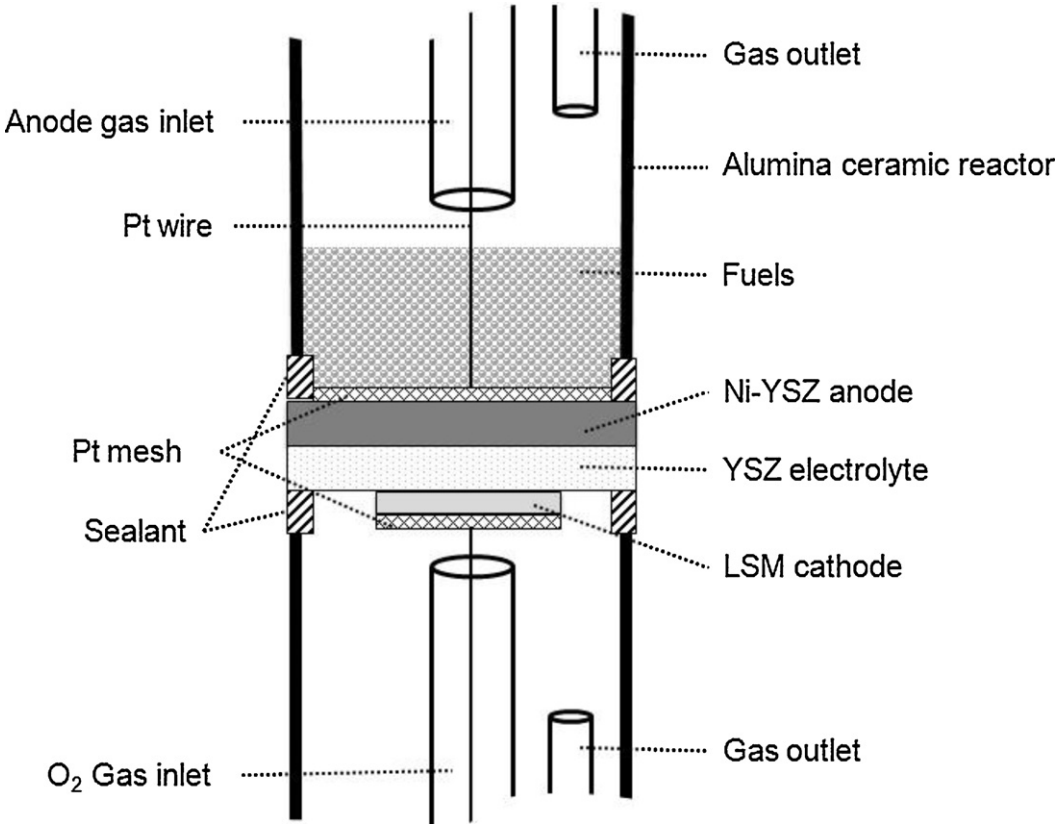

Fig. 2. Schematic diagram of a direct carbon fuel cell test system.

Sn-mixed carbon fuels to achieve the third fuel mixture. The Sn-mixed carbon fuels were dispersed by the aqueous impregnation of an $Ni(NO_3)_2{\cdot}6H_2O$ (Aldrich) solution. All mixtures were dissolved in 50 ml of deionized water and stirred for 5 h at 50 °C and then the samples were dried at 70 °C in an oven until obtaining a gel state, before being placed into the anode as a cylindrical pellet.

A schematic of the experimental DCFC unit is composed of an alumina ceramic reactor (NARA Cell-Tech, Korea), a furnace, and an electrochemical workstation (Scitech Korea, Korea), as shown in Fig. 2. Here, Pt mesh was used as a current collector and Pt paste (CL11-5100, Heraeus, US) was applied between the electrodes and Pt mesh to ensure good contact. The alumina ceramic reactor was heated to 900 °C at a rate of 5 °C min^{-1}. During heating, pure N_2 gas was provided at a flow rate of 30 ml min^{-1} in order to remove residual gas in the anode and pure O_2 gas was fed into the cathode at a flow rate of 100 ml min^{-1}. Once the desired operating temperature of 900 °C was achieved, power generation experiments were conducted and the resulting polarization curves were measured using the electrochemical workstation. The internal resistance of the cell was measured at a high frequency of 1 kHz using an AC-impedance meter (3560 AC mΩ HiTester, Hioki, Japan) [34]. In addition, the surface morphology of the cell was analyzed by field emission scanning electron microscopy (FE-SEM; S-4700, Hitachi, Japan) and the elemental qualitative analysis of the cell was carried out via energy dispersive X-ray spectroscopy (EDX; EMAX 7200-H, Horiba, England) coupled with FE-SEM. The crystallinity and elemental analysis of the cell were investigated using X-ray diffraction (XRD; MiniFlex II, Rigaku, Japan).

3. Results and discussion

In this DCFC based on a YSZ electrolyte, it is generally accepted that solid carbon fuels at the TPB react electrochemically with the oxygen ions emerging from the solid electrolyte (YSZ) and produce CO_2 and CO via simultaneously both 4- and 2-electron transfer reactions [4,14]:

$$C + 2O^{2-} \rightarrow CO_2 + 4e^- \quad (2)$$

$$C + O^{2-} \rightarrow CO + 2e^- \quad (3)$$

When CO is produced by reaction (3), CO can be further electrochemically oxidized to CO_2 as a gaseous fuel in the DCFC, as given by:

$$CO + O^{2-} \rightarrow CO_2 + 2e^- \quad (4)$$

In the DCFC with liquid Sn-mixed carbon, Sn metal can be electrochemically oxidized to SnO_2 at the anode:

$$Sn + 2O^{2-} \rightarrow SnO_2 + 4e^- \quad (5)$$

Fig. 3 shows the theoretical standard potentials as a function of temperature for possible carbon oxidations, calculated based on thermodynamic data [35,36]. The presence of only Sn powder in the DCFCs makes it possible to operate in metal-air battery mode. The theoretical open circuit voltage (OCV) for the oxidation of carbon (reactions (2) and (3)) and CO (reaction (4)) are higher than that of Sn when fuels are present in the anode. Sn/SnO_2 redox reactions may occur slowly. For this reason, Ni-based catalysts are generally used as anode materials for SOFCs. At temperatures above 750 °C, the dominant species are CO in thermal equilibrium, whereas at lower temperatures main gaseous species are CO_2 [8,14]. Since the direct electrochemical oxidation of solid carbon on the Ni–YSZ anode is thought to be intrinsically sluggish, Sn powder is introduced into carbon particles as an electrochemical mediator in order to promote accessibility of carbon fuels as well as oxygen ionic species from solid electrolyte.

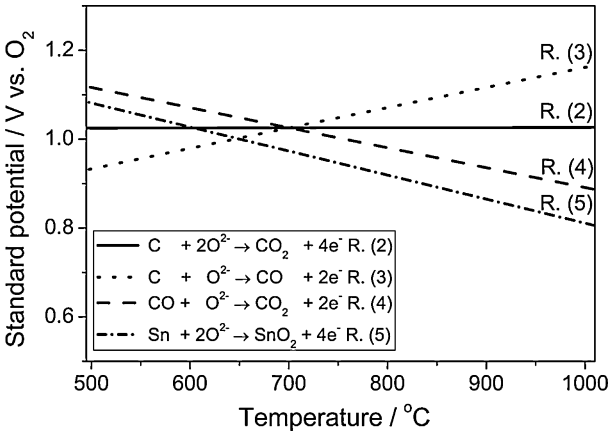

Fig. 3. Theoretical standard potentials (OCV) for possible anode reactions at various temperatures.

To investigate the effect of liquid Sn mixed in a solid carbon fuel on the DCFC performace, the polarization curves for the Ni–YSZ anode-supported button cells with Sn-free and Sn–carbon fuels were measured at 900 °C, as presented in Fig. 4. For the Sn-free fuel (pure carbon black), a sharp drop in cell voltage was observed at the beginning of the polarization curves (Fig. 4(a)). As expected, such drop indicates that the activation loss is caused by low activity for solid carbon and the slow electron transfer at the anode interface. The cells for Sn-free fuels exhibit a power density of only 14 mW cm^{-2}; this result is similar to recent studies that focus on the utilization of carbon fuels [22,23]. On the other hand, the

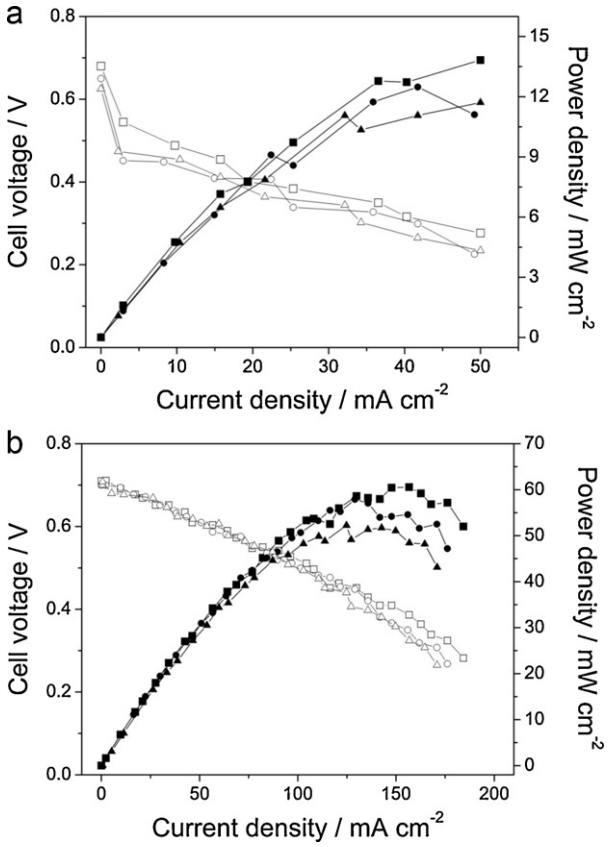

Fig. 4. Comparison of liquid Sn-mixed solid carbon fuels on polarization curves for (a) Sn-free (pure carbon black) and (b) Sn–carbon fuels at various gas flow rates at the anode: (■) without purging, (●) N_2 purge rate of 30 ml min^{-1}, and (▲) N_2 purge rate of 60 ml min^{-1}.

Table 1
Effect of temperature on OCV and high frequency resistance (HFR).

Temperature (°C)	Fuel			
	Sn-free fuel		Sn–carbon fuel	
	OCV (V)	HFR (Ω cm^2)	OCV (V)	HFR (Ω cm^2)
750	0.57	30	0.55	20
800	0.58	20	0.60	18
850	0.62	18	0.63	12
900	0.68	4.8	0.71	3.5

cells with Sn-mixed carbon fuel show significant improvements in performance and maximum power densities of 60.5 mW cm^{-2} are achieved. This result provides about 4 times higher power performance compared to that of the Sn-free fuel. Such enhancement of the DCFC performance indicates that the transfer of solid carbon particles and the kinetics of the electrochemical oxidation of carbon are facilitated by providing a better contact at the anode. In additon, increasing the anode gas flow rate for N_2 decreases the DCFC performance. When the anode is purged with N_2 gas, the partial pressure of the by-product CO (reaction (3)) might decrease due to the short residence time of the gases, possibly leading to inhibition of the CO oxidation reaction (reaction (4)); Li et al. [23] reported similar results in DCFC experiments by increasing the Ar gas flow rate.

The influence of temperature on the OCV and the internal resistance of the cell were then investigated by measuring a high frequency resistance, as shown in Table 1. The measured OCV increases with an increase of operating temperature and the cell resistance decreases significantly. In general, for high ionic conductivity in solid electrolytes of SOFCs such as YSZ, the operating temperature must be greater than at least 700 °C [26]. The contact resistance of both cases, however, is much higher than the value predicted on the basis of electrolyte thickness, even though the cell temperature reaches 900 °C. In addition, there is also a wide difference between the theoretical and experimental values in OCV. Nevertheless, a higher OCV and lower contact resistance can be obtained with Sn–carbon fuel in this study. At higher temperatures, Sn is turned into liquid state due to its low melting point of 232 °C. As such, the porous anode layer will be effectively linked with liquid Sn, which could enhance the physicochemical contact between fuel-to-anode and anode-to-current collector.

Fig. 5 shows the XRD patterns of the Ni–YSZ anode for the as-prepared and after-tested cells. Various crystalline diffraction peaks corresponding to Ni (1 1 1), Ni (2 0 0), and NiO (1 1 1) are observed, and the intensity of their diffraction peaks is relatively increased after DCFC operation. In particular, in the tested anode with Sn–carbon fuels (Fig. 5(c)), the polycrystalline intensity peaks corresponding to SnO_2 (1 1 0) at 26.61°, (1 0 1) at 33.89°, and (2 1 1) at 51.78° are observed. Sn is thought to be slightly consumed by the electrochemical oxidation reaction (reaction (5)). Thus, the peaks can be assigned to the oxide formation of Sn. Fig. 5(d)–(f) presents an photograph, SEM image, and EDX data of the Ni–YSZ anode after *I–V* test with Sn–carbon fuels. A slight SnO_2 layer (white color) formed on the anode and the EDX data confirmed the presence of Sn-mixed carbon fuels capable of penetrating more deeply into Ni–YSZ anode layer due to formation of the liquid Sn state.

Long term stability of the Ni catalyst is governed by its ability to selectively oxidize carbon while preventing the rapid growth of carbon deposits which poison the catalyst. Nikolla et al. [37,38] reported that Sn–Ni alloys have a higher propensity to oxidize carbon and are much more carbon-tolerant than pure Ni. Fig. 6 shows the polarization curves of the DCFCs at 900 °C obtained while introducing CO gas, in which maximum power densities are 20 and 200 mW cm^{-2} for Sn-free and Sn–carbon fuels, respectively. Therefore, it is fair to say that Sn in the mixed fuels with Ni–YSZ anode also plays an important role in controlling Ni surface, thereby mitigating poisonous carbon deposit formation. In addition, such a dramatic

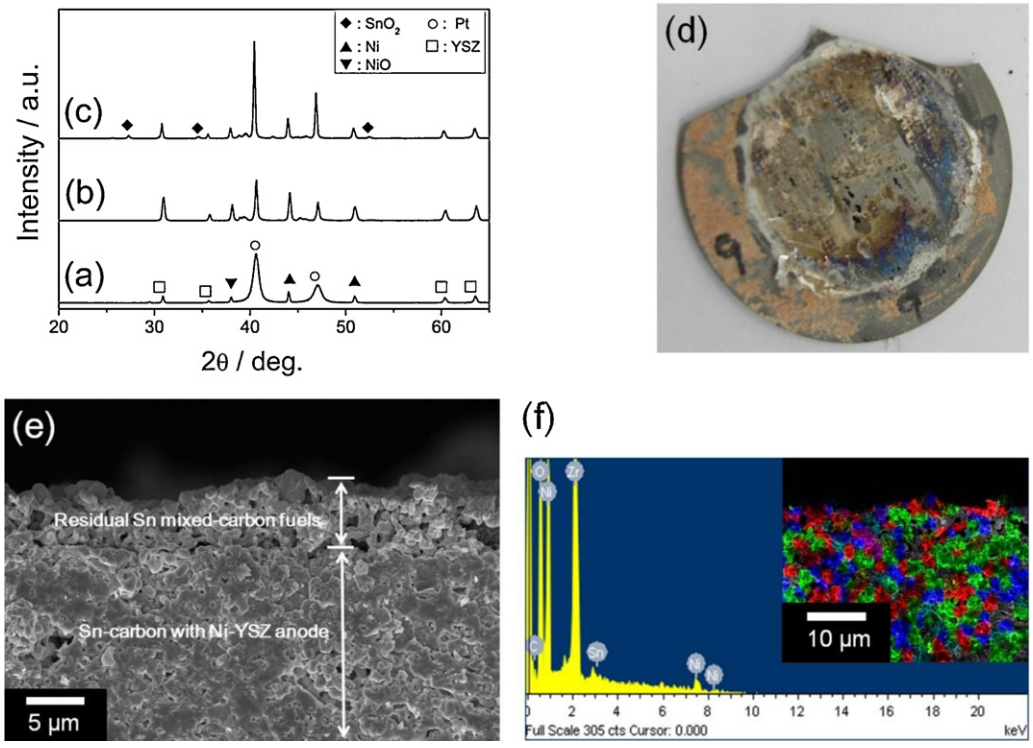

Fig. 5. Comparison of XRD patterns of Ni–YSZ anodes: (a) as-prepared anode and after-tested anode (b) with Sn-free and (c) Sn–carbon fuels. (d) Photo image of MEA surface, (e) cross-sectional SEM image, and (f) X-ray elemental color map with EDX analysis of after-tested anode with Sn–carbon fuels (Ni is green, Sn is red, carbon is blue, and other elements are black). (For interpretation of the references to color in this figure legend, the reader is referred to the web version of the article.)

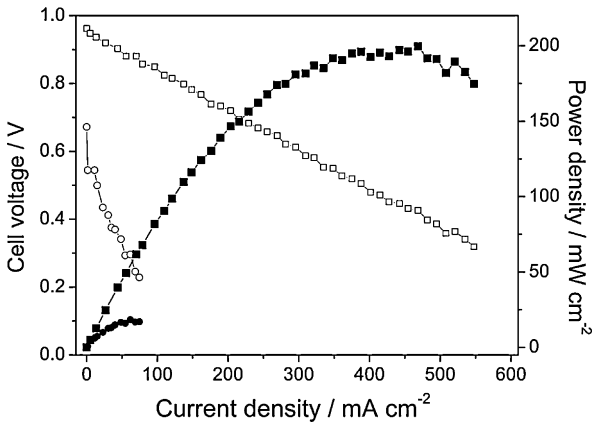

Fig. 6. Effect of activity for CO gas (30 ml min^{-1}) oxidation in anode fuels on polarization curves for (■) Sn-free and (●) Sn–carbon fuels.

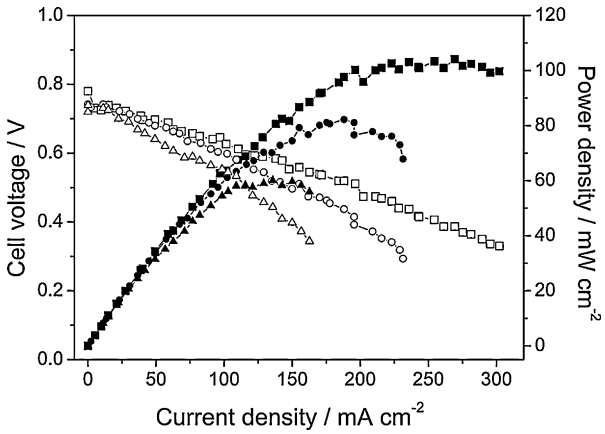

Fig. 7. Effect of an additional Ni catalyst-impregnated Sn–carbon fuels on polarization curves at various gas flow rates at the anode: (■) without purging, (●) N_2 purge rate of 30 ml min^{-1}, and (▲) N_2 purge rate of 60 ml min^{-1}.

increase in cell performance is partially attributed to the fact that a liquid Sn anode provides good catalytic activity for CO as well as carbonaceous fuel oxidation [30,31].

Furthermore, transition metals loaded onto the carbon fuels have been known to show several times higher performance than those using only solid carbon fuels [39,40]. In particular, an obvious implication of the above results is that adding Ni metal to Sn–carbon mixtures will promote the chemical as well as electrochemical oxidation reaction. Fig. 7 shows the polarization curves for DCFCs with the Ni-impregnated Sn–carbon fuel at 900 °C. The addition of Ni metal enables us to increase in the cell performance from 80 to 105 mW cm^{-2} under N_2 purging. The most probable scenario could be that Ni (or Ni oxide) in the Sn–carbon mixtures enhance the chemical oxidation of C toward CO and then Ni–YSZ anode with Sn could also accelerate the electrochemical oxidation of CO to CO_2 (reactions (4)).

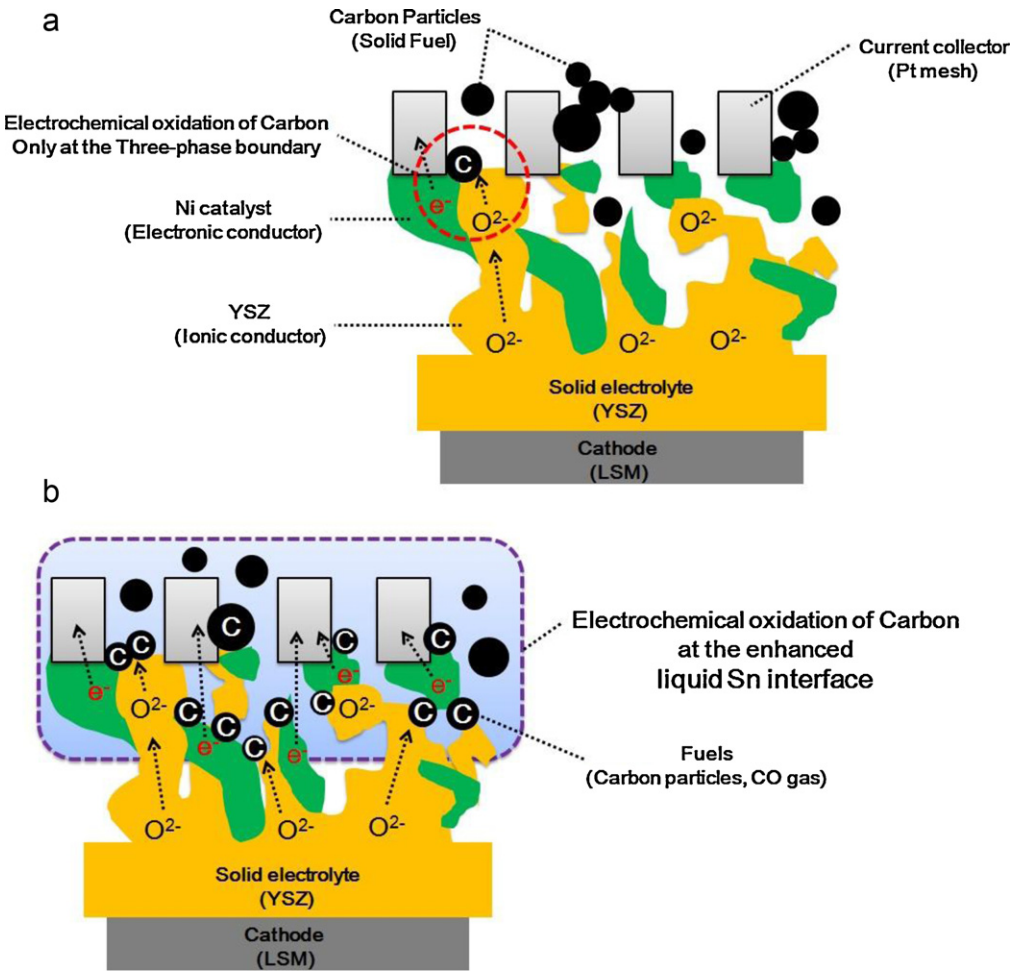

Fig. 8. Schematic representation showing Ni–YSZ anode in DCFCs. Electrochemical oxidation of solid fuels can occur at the TPB with oxygen ions emerging from the solid electrolyte and to produce CO_2 and CO. (a) Typical Ni–YSZ anode and (b) enhanced liquid Sn anode interface.

Finally, we summarize the role of liquid Sn in mixed fuels. A schematic illustration of the plausible mechanism is also presented in Fig. 8. First of all, Sn in the mixed fuels can convey carbon fuels into certain depth of Ni–YSZ anode layer, thereby not only increasing the surface area between two solid phases but also shortening the pathway of ionic species to reaction sites. Sn is also capable of promoting electrochemical oxidation of carbon and/or carbon monoxide by alleviating carbon deposit formation on the Ni catalyst surface. Lastly, Sn metal can be electrochemically oxidized to SnO_2 at the anode, according to Eq. (5).

4. Conclusion

A DCFC system was successfully developed by applying Sn powder mixed with carbon black. The Sn in the mixed carbon fuels plays major roles in (i) building a favorable bridge between the solid fuel-to-solid anode and (ii) facilitating the electrochemical oxidation of carbon to CO and CO_2. Moreover, an additional loading of Ni in the Sn–carbon fuels, further improvement of the DCFC can be achieved by improving the chemical oxidation of carbon for producing CO which can be readily converted to CO_2 electrochemically. Finally, it is anticipated that future research will be more focused on the long-term durability by optimizing the catalytic activity of electrochemical mediators as well as auxiliary catalysts in carbon fuels with Ni–YSZ anode. Furthermore, a novel concept for a continuous fuel supply is quite necessary to realize a practical fuel cell system.

Acknowledgement

This work was supported by the Core Technology Development Program for Next-generation Energy Storages of Research Institute for Solar and Sustainable Energies (RISE), GIST.

References

[1] IEA, World Energy Outlook 2010, IEA, Paris, 2010.
[2] BP, BP Statistical Review of World Energy, BP, London, 2010.
[3] B. Heydorn, S. Crouch-Baker, Fuel Cell Rev. 2 (2006) 15–21.
[4] M. Ihara, S. Hasegawa, J. Electrochem. Soc. 153 (2006) A1544–A1546.
[5] D. Cao, Y. Sun, G. Wang, J. Power Sources 167 (2007) 250–257.
[6] H.C. Howard, Direct Generation of Electricity from Coal and Gas (Fuel Cells), John Wiley and Sons, New York, 1945.
[7] W.W. Jacques, US Patent No. 555,511 (1896).
[8] S. Zecevic, E.M. Patton, P. Parhami, Carbon 42 (2004) 1983–1993.
[9] G.A. Hackett, J.W. Zondlo, R. Svensson, J. Power Sources 168 (2007) 111–118.
[10] N.J. Cherepy, R. Krueger, K.J. Fiet, A.F. Jankowski, J.F. Cooper, J. Electrochem. Soc. 152 (2005) A80–A87.
[11] D.G. Vutetakis, D.R. Skidmore, H.J. Byker, J. Electrochem. Soc. 134 (1987) 3027–3035.
[12] X. Li, Z. Zhu, J. Chen, R. de Marco, A. Dicks, J. Bradley, G. Lu, J. Power Sources 186 (2009) 1–9.
[13] N. Nakagawa, M. Ishida, Ind. Eng. Chem. Res. 27 (1988) 1181–1185.
[14] M. Ihara, K. Matsuda, H. Sato, C. Yokoyama, Solid State Ionics 175 (2004) 51–54.
[15] S. Hasegawa, M. Ihara, J. Electrochem. Soc. 155 (2008) B58–B63.
[16] H. Saito, S. Hasegawa, M. Ihara, J. Electrochem. Soc. 155 (2008) B443–B447.
[17] Y. Wu, C. Su, C.M. Zhang, R. Ran, Z.P. Shao, Electrochem. Commun. 11 (2009) 1265–1268.
[18] T.M. Gür, R.A. Huggins, J. Electrochem. Soc. 139 (1992) L95–L97.
[19] T.M. Gür, J. Electrochem. Soc. 157 (2010) B751–B759.
[20] T.M. Gür, M. Homel, A.V. Virkar, J. Power Sources 195 (2010) 1085–1090.
[21] S. Li, A.C. Lee, R.E. Mitchell, T.M. Gür, Solid State Ionics 179 (2008) 1549–1552.
[22] J.-P. Kim, H. Lim, C.-H. Jeon, Y.-J. Chang, K.-N. Koh, S.-M. Choi, J.-H. Song, J. Power Sources 195 (2010) 7568–7573.
[23] C. Li, Y. Shi, N. Cai, J. Power Sources 196 (2011) 4588–4593.
[24] A.M. Posner, Fuel 34 (1955) 330–338.
[25] D.B. Weibel, R. Boulatov, A. Lee, R. Ferrigno, G.M. Whitesides, Angew. Chem. Int. Ed. 44 (2005) 5682–5686.
[26] S. Mclntosh, R.J. Gorte, Chem. Rev. 104 (2004) 4845–4865.
[27] I.V. Yentekakis, P.G. Debenedetti, B. Costa, Ind. Eng. Chem. Res. 28 (1989) 1414–1424.
[28] S. Gopalan, G. Ye, U.B. Pal, J. Power Sources 162 (2006) 74–80.
[29] T. Tao, L. Bateman, J. Bentley, M. Slaney, ECS Trans. 5 (2007) 463–472.
[30] T. Tao, M. Slaney, L. Bateman, J. Bentley, ECS Trans. 7 (2007) 1389–1397.
[31] T. Tao, W. Mcphee, M. Koslowske, L. Beteman, M. Slaney, J. Bentley, ECS Trans. 12 (2008) 681–690.
[32] G. Sikha, W. Mcphee, Q. Zhang, M. Koslowske, T. Tao, R. White, ECS Trans. 17 (2009) 161–173.
[33] T. Tao, W. McPhee, M. Koslowske, J. Bentley, M. Slaney, L. Beteman, ECS Trans. 25 (2009) 1115–1124.
[34] S. Uhm, Y. Kwon, S.T. Chung, J. Lee, Electrochim. Acta 53 (2008) 5162–5168.
[35] D.R. Lide (Ed.), CRC Handbook of Chemistry and Physics, 84th ed., CRC Press LLC, 2003–2004, pp. 61–84 (Section 5).
[36] M. Iwase, M. Yasuda, S. Miki, T. Mori, Trans. Jpn. Inst. Met. 19 (1978) 654–660.
[37] E. Nikolla, A. Holewinski, J. Schwank, S. Linic, J. Am. Chem. Soc. 128 (2006) 11354–11355.
[38] E. Nikolla, J.W. Schwank, S. Linic, Catal. Today 136 (2008) 243–248.
[39] Y. Nabae, K.D. Pointon, J.T.S. Irvine, J. Electrochem. Soc. 156 (2009) B716–B720.
[40] Y. Tang, J. Liu, Int. J. Hydrogen Energy 35 (2010) 11188–11193.